

Iranian Journal of Oil & Gas Science and Technology, Vol. 11 (2022), No. 2, pp. 1–18
http://ijogst.put.ac.ir

Detection of Heavy bitumen Contaminations with Using Corrected Rock-Eval Pyrolysis Data

Meisam Hemmati¹, Yaser.Ahmadi^{2*}

¹M.S. Student, School of Geology, College of Science, University of Tehran, Tehran, Iran.

²Assistant Professor, Chemical and Petroleum Engineering Department, Ilam University, P.O. Box 69315/516, Ilam, Iran.

Highlights

- Application of the S₂ versus TOC graph in the detection of in-situ bitumen contamination.
- Evaluating the accuracy of geochemistry data obtained from the Rock-Eval pyrolysis apparatus.
- The y-intercept in the graph of S₂ versus TOC.
- Determining depositional system tracts using the graph of S₂ versus TOC.

Received: June 21, 2021; revised: August 06, 2021; accepted: August 20, 2021

Abstract

The Rock-Eval pyrolysis is a thermal method that is widely used by the petroleum geologist for evaluation of source rock characteristics and obtain geochemistry parameters. However, there are misconceptions and misuses in exceptional cases that could lead to erroneous conclusions after using the Rock-Eval pyrolysis data to evaluate the properties of organic matter. However, a cross-plot of S₂ (petroleum potential) versus TOC (total organic carbon) is the usable tool to solve issues and applied for checking the accuracy of the geochemistry parameters. The graph provides the correction criteria for the S₂, HI (hydrogen index), and kerogen type. As well as, the graph measures the adsorption of hydrocarbon by the mineral matrix. In addition, this article demonstrates a manner based on the data plot of S₂ versus TOC to detect bitumen or hydrocarbon contaminations. Based on our knowledge about the Garau Formation as a possible source rock in petroleum geology of Iran, a geochemistry study by Rock-Eval VI pyrolysis and Leco Carbon Analyzer has been conducted on many rock samples collected from different outcrops in the Lurestan province, Aligudarz region, from South-West of Iran, High Zagros. Plotting the data on a cross plot of S₂ versus TOC, drawing the regression line, and finding the regression equation are the best method for determining the real values of S₂ and HI parameters and bitumen/hydrocarbon contamination. Contamination creates a y-intercept in the graph of S₂ versus TOC which makes geochemistry data unreliable in two study location. As, led to the S₂ and HI data unrealistically increased, while the Tmax values went down and reduced the thermal maturity of the organic matters from its real status. For skipping the effect of contamination and obtaining the real geochemistry parameters, the y-intercept of the graphs removed and the corresponding values subtracted from the HI and S₂. The cause of contamination in the Garau Formation is the adhesion of heavy bitumen to organic facies due to the covalent bonds between carbon and hydrogen ions.

Keywords: Rock-Eval pyrolysis, Heavy bitumen contamination, Geochemistry, Sedimentary system tracts

How to cite this article

Hemmati .M, Ahmadi. Y, *Detection of Heavy Bitumen Contaminations with Using Corrected Rock-Eval Pyrolysis Data, Iran J. Oil Gas Sci. Technol., Vol. 11, No. 2, p.1-18, 2022. DOI:10.22050/ijogst.2021.290550.1598*

* Corresponding author :

Email: yaser.ahmadi@ilam.ac.ir

1. Introduction

Petroleum geochemistry is an established science that improves exploration and production efficiency and it has been characterized as a mature science for increasing the chances of success in oil exploration (Bordenave, 1993; Miller, 1995; Peters and Fowler, 2002). Petroleum geologists should check the accuracy of the data before interpretation, and this fact decreases the risk of projects and the possibility of dealing with unexpected cases and even reduce irreparable costs. Obtaining geochemistry data by the Rock-Eval pyrolysis is a quick, low-cost, and most applied technique for evaluating petroleum generation potential of source rocks, and it provides information on the quantity, type, and thermal maturity of the associated organic matter (Espitalie, 1977; Peters, 1986). Petroleum potential of source rocks is related to its organic carbon content, and the total organic carbon (TOC) analysis is the first screening analysis methods for evaluating the general hydrocarbon potential (Jarvie, 1991; Tissot and Welte, 1984).

In the cross-plots of S₂ versus TOC, there is a linear function between TOC, S₂, and HI values (Clayton and Ryder, 1984; Langford and Valleron, 1990). The hydrogen index derived from the regression line in the such cross-plot can measure the average HI of the organic matter that are pyrolysable (Dahl et al., 2004; Maky et al., 2010). When the regression line is not intersecting at the origin of the graph, the total HI according to the slope of the curve (regression line), is different from the arithmetic mean of the HI. In cases were $y_0 = 0$ and the regression line intersects the origin, the HI derived from arithmetic mean or the slope of the curve, are close to each other (Dahl et al., 2004). In other cases, when regression line doesn't pass through the origin of the graph, there is x-intercept or y-intercept.

Previous reports reveals that the Garau Formation is a known as potential and effective source rock in south-west of Iran (Bordenave and Burwood, 1990; Bordenave and Hegre, 2010), and most probably it charged limited reservoirs in that region (Bordenave and Hegre, 2005). Based on the need of further geochemistry studies about the Garau Formation, especially its hydrocarbon-generation potential, in the current study, the geochemistry parameters were obtained by Rock-Eval apparatus and the carbon analysis was done by the LECO technique. In this research geochemistry analyses have applied on five outcrop rock samples of the Garau Formation, and the accuracy of geochemistry data has evaluated to create a criterion accuracy of geochemistry data.

2. Geological setting and stratigraphy

The Zagros orogenic belt is limited to the Zagros reverse fault in northeast and to Dezful embayment in southeast, which Lurestan depression was located in northwest part of it. Many reservoirs and source rocks have been detected in this region, and the Garau Formation is one of the most effective source rocks of this region (Bordenave and Burwood, 1990). The Garau Formation's type section has been defined on the southwestern flank of Kabir Kuh in southwestern Lurestan near the Qaleh Darreh village. The Garau Formation underlies the Sarvak Formation in its type section and From Lurestan zone toward Dezful embayment and Fars's basin this Formation gradually passes into carbonate platform strata of the upper Khami Group, and its lithological and geochemical characteristics varies in other regions (Bordenave and Burwood, 1990). The formation's age in its type section is related to the Neocomian to Coniacian (Wynd, 1965). However, the age of the upper part of this formation is also attributed to upper Toronian (Alavi, 2004; Bordenave and Burwood, 1990) or Aptian, Albian (Al-Husseini and Moujahed, 2000). These differences seem to be related to related to the location of the study. The Garau Formation is composed of low energy facies locally pyritic, argillaceous lime micritic limestone (mudstone) and dark gray to black, organic matter rich bioclastic shale (Alavi, 2004). The Garau Formation overlies the Gotnia evaporites in Lurestan Basin, deposited in deeper parts of a continental shelf, and is time equivalent of the Gadvan, Kazhdumi and Dariyan Formations in other regions of Iran (Alavi, 2004;

Ghazban and Motiei, 2007). The thickness of the formation is about 624 m in its type section (Ghazban and Motiei, 2007). In study area, the Garau intervals characterized by large lateral variation in thickness, showing at some localities' pinch and swell structures. Figure 1 shows the study area with its tectonic elements and Figure 2 is a schematic stratigraphy chart of Lurestan basin in Zagros orogeny belt.

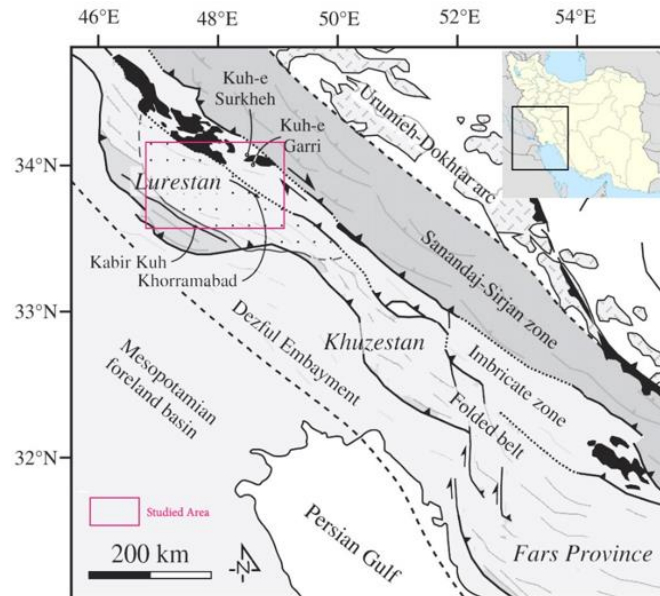


Figure 1

Structural setting of the Zagros fold-thrust-belt showing the study area situations (Homke et al., 2009).

Schematic Stratigraphy of SW Iran (Lurestan)			
Age	Formation	Lithology	Description
Lower Cretaceous	Garau	[Pattern: Horizontal lines]	Mainly argillaceous limestone with black shales
		[Pattern: Dotted]	Altered limestone with anhydrite intercalation
Upper Jurassic	Gotnia	[Pattern: Dotted]	Mainly oolitic limestone
	Najmeh	[Pattern: Wavy lines]	
Middle Jurassic	Sargelu	[Pattern: Horizontal lines]	Black radiolaria bearing shales and argillaceous carbonates

Figure 2

The schematic stratigraphy of Lurestan basin (modified after Motiei, 1993).

3. Materials and methods

3.1. Sampling

In this study, 123 outcrop rock samples have collected from the organic matter-rich facies of the Garau Formation in five locations (A, B, C, D, and E) in Lurestan province, south-west of Iran, High Zagros. In each location, the samples were systematically collected from the base to top of the intervals, with vertical sampling distance of 1.5 m. The possible surface alterations were eliminated before using. For direct measurement of TOC using LECO method, the sample were primarily treated with HCl and HF solutions to remove carbonate and silicates (Hunt, 1996; Tyson, 1995).

3.2. Leco carbon analyzer

In the Leco method, the organic carbon is combusted without the intervention of mineral carbon (e.g., carbon in argillaceous limestone or clay samples), so the determination of total carbon by the Leco method is better than calculation by Rock-Eval pyrolysis, especially for carbon-rich samples. So, samples were first crushed, and then according to the method mentioned above, are acid treated. After that, they combusted at about 1000 °C using a high-frequency induction furnace in an oxygen atmosphere using a LECO CR-412 apparatus. Next, the carbon contained in the kerogen was converted to CO and CO₂. Finally, the evolved carbons were measured in an infrared cell and converted to TOC (Bernard, 2010; Peters, 1986).

3.3. Rock-eval pyrolysis

The Rock-Eval VI analysis was performed to obtain geochemical parameters. The Rock-Eval pyrolysis uses temperature programmed heating of a small amount of rock (100 mg) in an oxygen-free atmosphere (helium or nitrogen). The generated liquid hydrocarbons are recorded in peaks as S1 (free hydrocarbon; mg HC/g rock), S2 (cracked hydrocarbon; mg HC/g rock), S3 (derived from oxygen containing organic molecules; mg CO₂/g rock) (Espitalié, 1985a, 1985b, Espitalié, et al., 1977). Other important measurements include Tmax, hydrogen and oxygen indices (HI and OI) (Peters, 1986).

3.4. The S2 versus TOC diagram

Plotting the data on the graph of S2 versus TOC, and drawing the regression line, is a usable tool to determine real geochemistry parameters, such as HI, production index (PI=S1/S1+S2), kerogen type, and main expelled products. Another important usage of cross-plot is to detect mineral matrix effect and bitumen or hydrocarbon contamination, according to x-intercept and y-intercept created on the graph, respectively (Langford and Valleron, 1990; Dahl et al., 2004). As, the data must first be plotted. Then, the regression line should be drawn and to acquire the line equation. The line equation is a first-order equation such as equation 1 and 2 (Thomas et al., 2016):

$$y=mx\pm y_0 \quad (1)$$

$$S_2=m\text{TOC}\pm y_0 \quad (2)$$

The slope of the regression line (m) is equal to the $\tan\alpha$, which represents the HI. As well as, the constant number (y₀) is the intersection from the origin that is the representative of underestimation (-y₀), and overestimation (+y₀) in the S₂ or HI when the x-intercept and y-intercept induced, respectively. On one hand, the high organic matter contents in the source rock yields low products, and on contrary the low contents organic matters produce higher products. In other word, when y₀=-b, there is x-intercept and when y₀=+b, there is y-intercept. The intersection from X-axis represents the average amount of inert or dead organic carbon (Dahl et al., 2004) or mineral matrix effect in the analyzed sections (Langford and Valleron, 1990). This means that a threshold amount of organic material must be present before enough hydrocarbons can be detected during pyrolysis (Erik et al., 2006). On the other hand, the

intersection from the Y-axis represents unreal HI which emerge by in-situ bitumen or oil contaminations. Locations A and C with contaminated samples have been revised to remove the effect of contamination. To acquire the real S₂ and other parameters associated with it, such as HI and PI, the y-intercept should be eliminated. Hence, the following equations are innovated:

$$\text{Real } S_2 = S_2 - y_{\text{intercept}} \quad (3)$$

$$\text{Real HI} = \text{Real } S_2 / \text{TOC} \times 100 \quad (4)$$

$$\text{Real PI} = S_1 / S_1 + \text{Real } S_2 \quad (5)$$

In a similar manner, for the cases with mineral matrix effect that happened in the B, D, and E location samples, the real S₂ and other geochemical parameters could gain by adding x-intercept values to the measured S₂ from the Rock-Eval pyrolysis, as follow:

$$\text{Real } S_2 = S_2 + y_{\text{intercept}} \quad (6)$$

4. Result and discussion

4.1. Total Organic Carbon (TOC) and pyrolysis parameters

Table 1 indicate all relevant geochemical data in this study. The Leco Carbon Analyzer shows the TOC% ranging between 0.3 to 26.4 wt. % with average of 14.71wt. %. The HI ranges from 93 to 762 with average of 542.42 (mg HC/gr TOC) (highest in locations A and C). As well as, the OI has values of 2 to 258 with average of 14.67 (mg CO₂/g TOC), indicates predominantly oil-prone kerogen type I and some type II as shown in the figure 3. The S₁ ranges from 0.1 to 4.71 with an average of 1.62 mg HC/g rock, as well as the S₂ values are between 0 to 140.2 with average of 82.54 mg HC/g rock (highest in A and C locations). The geochemistry parameters indicate the quality of source rock is excellent (Peters, 1986; Peters and Cassa, 1994). The measured T_{max} is between 423°C to 441°C which means the samples are thermally immature or early mature (Peters and Cassa, 1994), or marginally entered the beginning of oil window (Peters, 1986; Rimmer et al., 1993). It should be noted that the low values of S₁ are due to doing sampling from outcrops which affected by surface weathering and hydrocarbon evaporations.

Table 1

Results from Rock–Eval Pyrolysis of investigated rock samples.

Location name	S ₁ (Mg HC/g rock)	S ₂ (Mg HC/g rock)	S ₃ (Mg CO ₂ /g rock)	TOC (wt.%)	T _{max} (°C)	S ₂ /S ₃	HI (Mg HC/gr TOC)	OI (Mg CO ₂ /g TOC)	PP (mg HC/gr TOC)	PI	
A	1.8	91.7	1.3	15.9	432.1	92.9	588.0	8.4	93.4	0.02	
Average	4.7	138.7	4.0	25.7	437.0	289.6	762.0	25.0	142.4	0.04	
Maximum	0.2	44.5	0.4	8.1	426.0	21.7	442.0	2.0	44.9	0.00	
Minimum	B	0.5	38.4	0.8	7.1	433.5	30.6	449.3	26.8	38.9	0.02

Average	3.3	139.6	2.1	24.2	438.0	77.5	621.0	57.0	142.8	0.05
Maximum										
Minimum	0.0	1.4	0.3	0.6	431.0	4.7	213.0	7.0	1.4	0.00
C	1.7	90.5	1.7	16.4	431.8	61.9	555.2	10.6	92.2	0.02
Average	2.5	111.6	3.5	19.4	436.0	106.2	611.0	20.0	114.1	0.03
Maximum										
Minimum	0.6	66.0	1.0	10.8	429.0	23.4	479.0	5.0	66.7	0.01
D	1.0	67.0	1.1	12.4	431.0	61.9	478.7	39.2	68.0	0.02
Average	2.1	115.9	2.7	21.4	436.0	126.4	576.0	258.0	117.3	0.06
Maximum										
Minimum	0.0	0.3	0.6	0.3	427.0	0.4	106.0	4.0	0.4	0.01
E	2.1	82.6	1.4	15.5	431.0	73.2	497.0	14.6	84.7	0.03
Average	4.6	140.2	2.8	26.4	441.0	222.5	667.0	56.0	144.8	0.18
Maximum										
Minimum	0.1	1.2	0.5	1.3	423.0	1.7	93.0	2.0	1.4	0.01

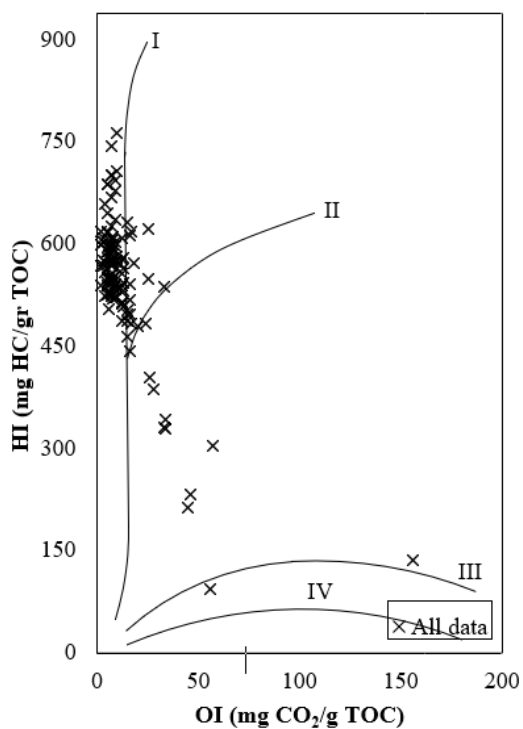


Figure 3

Cross-plots of HI versus OI show the presence of kerogen type I, I/II and II (Hunt, 1996).

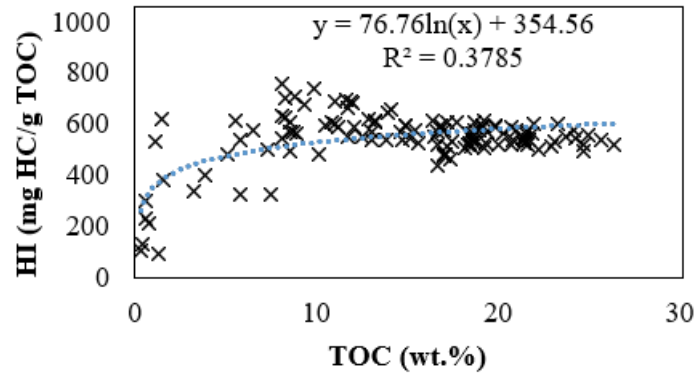
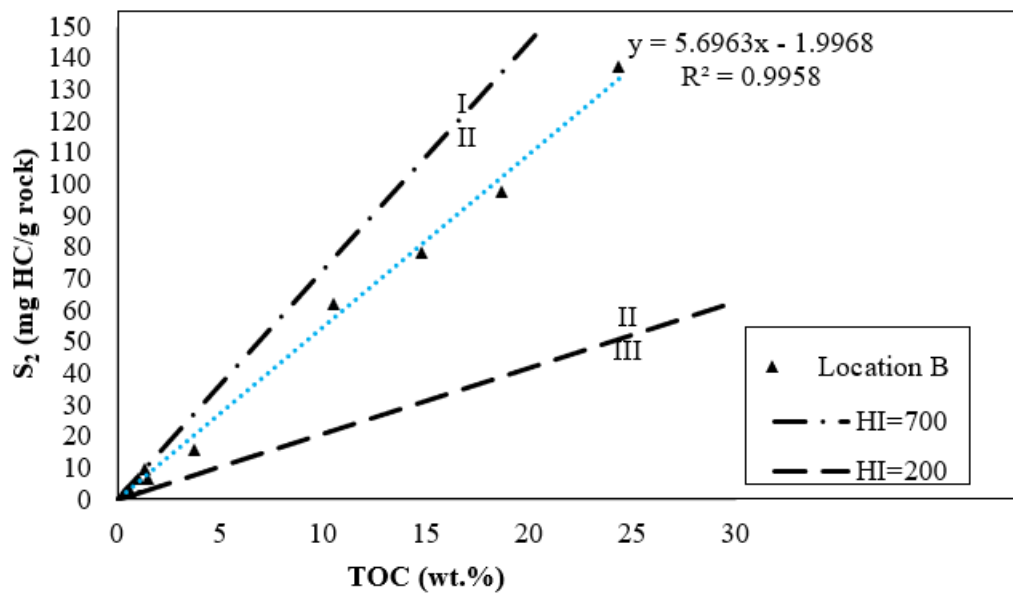
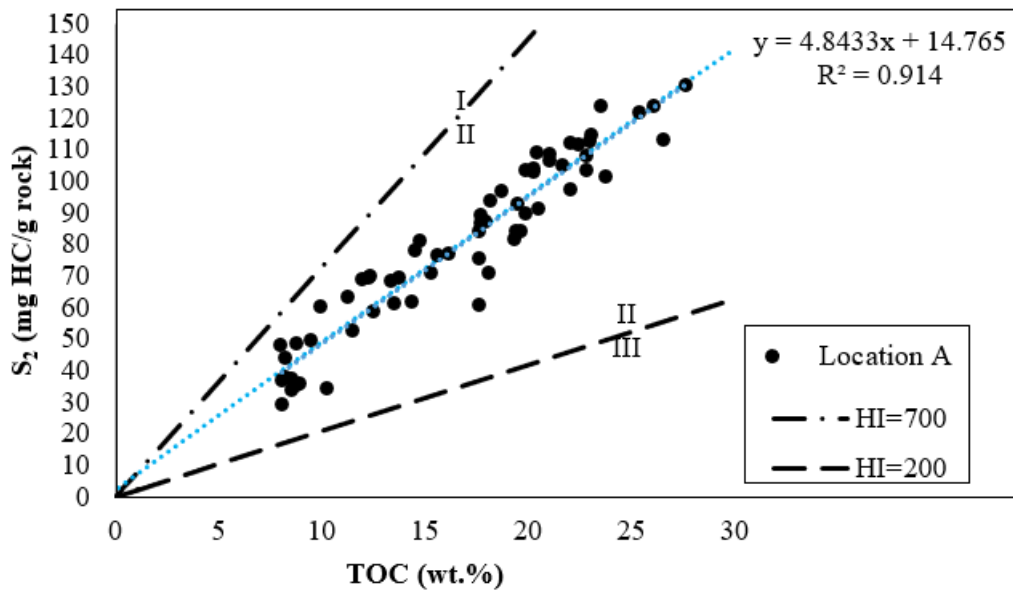
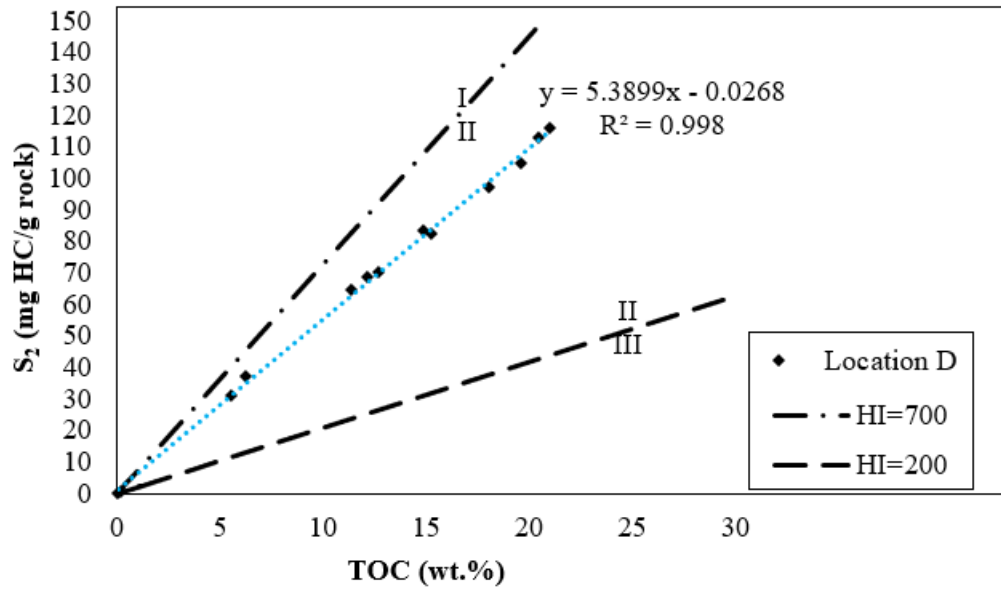
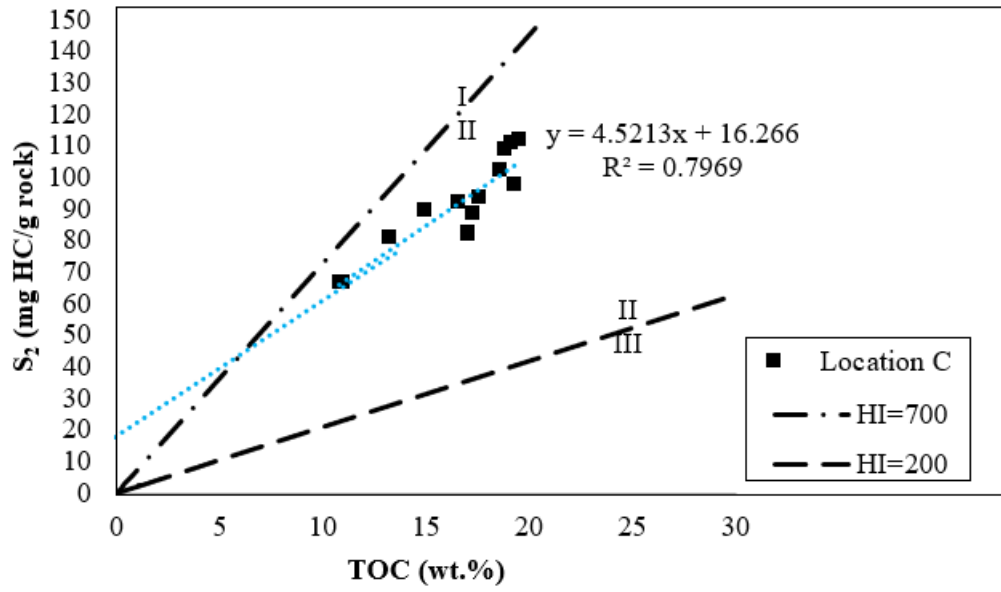


Figure 4

The HI versus TOC cross-plot to investigate relationship between products and organic matter.





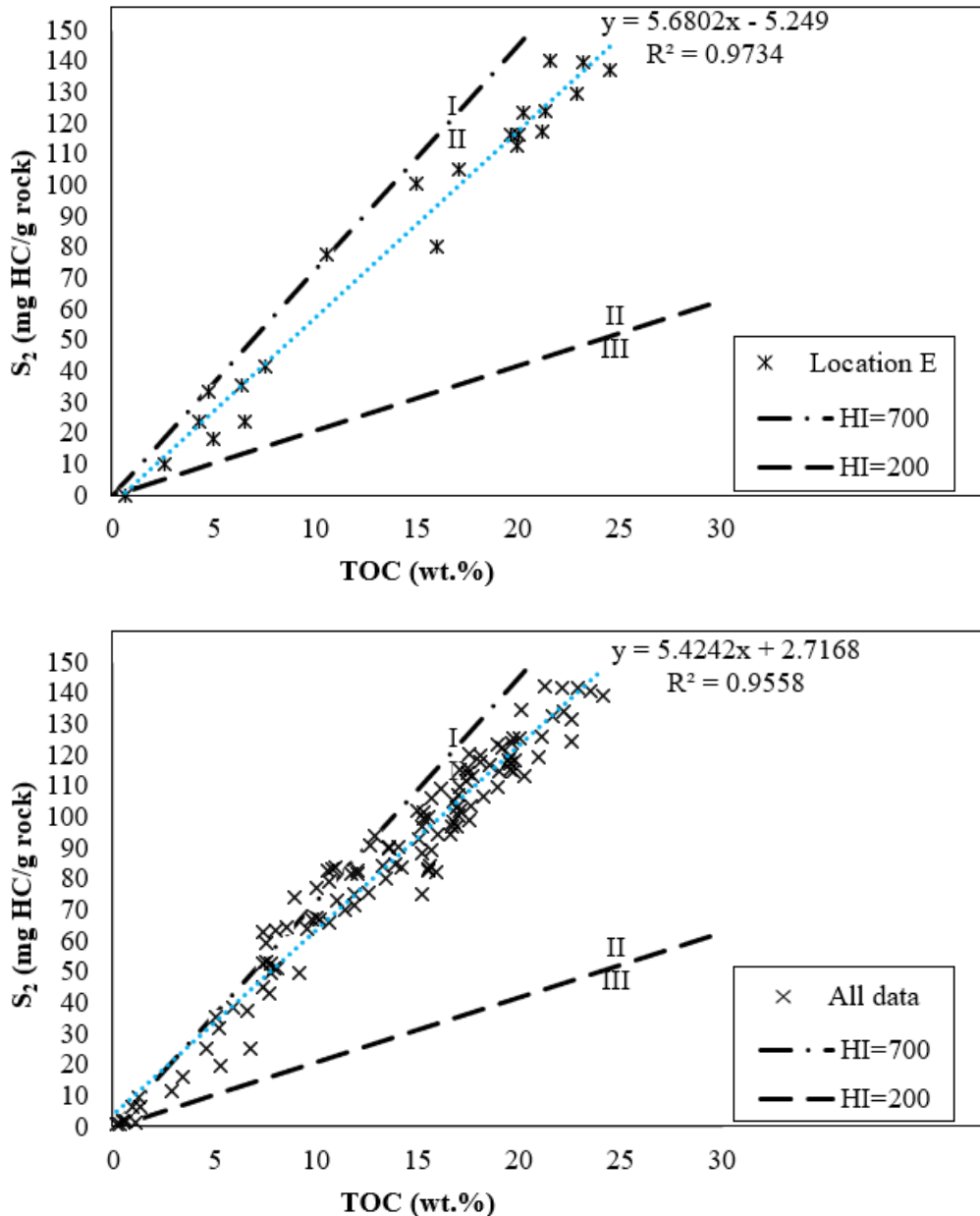


Figure 5

The S₂ versus TOC cross-plot indicate y-intercept in locations A and C, showing bitumen contamination (Langford and Valleron, 1990).

Since the HI versus OI cross-plots (Figure 3) doesn't show the presence of inert kerogen, whereas reveals the oil-prone kerogens, then the x-intercept in the B, D, and E locations created by the mineral matrix effect. Nevertheless, according to the regression line for all data plot in the figure 5, the samples affected by the matrix effect are very lower than the contaminated samples. As well as, the two agents can be detected for creating that abnormal situation in the A and C locations; first is the in-situ bitumen contamination in the source rock, and the second reason is immigration to the source rock. According to the figure 6, the free hydrocarbons (S1) are indigenous and produced by maturation of the organic matter of the source rock, and no external agent such as immigration interfered in contamination of the Garau Formation (Espitalie et al., 1977; Hunt, 1996). The covalent bonding between hydrogen and carbon ions in the heavy bitumen of the Garau Formation caused the generated products to adhere the

surface of organic facies. Then, the heavy bitumen remains in the source rock even at high temperatures and have not expelled easily. Eventually, the in-situ contamination has occurred (Morrison and Boyd, 1992; Mortimer, 1986).

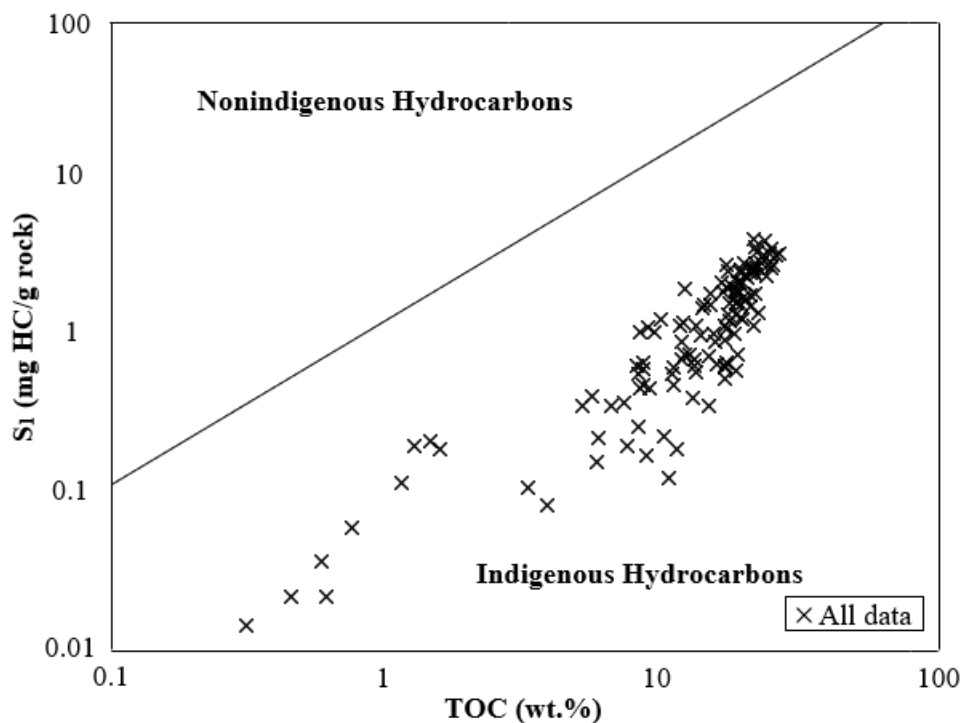


Figure 6

S₁ versus TOC cross-plot, to find out migration from immigration (Hunt, 1996).

The calculated HI from contaminated samples by the Rock-Eval pyrolysis and without making any appropriate corrections, usually are not represent the true HI. Such uncorrected data will induce scattered plots and interception on the Y-axis in the graphs of HI versus TOC, and S₂ versus TOC. The y-intercept when induced that the samples with high HI or S₂ associated with low TOC. The contamination caused the S₂ and HI values to increase unrealistically, and to decrease the T_{max} from its real values (Peters, 1986). In such situations, the thermal maturation occurs earlier and the peak of S₂ appears more easily. Then, the real thermal maturity in the contaminated samples will be higher than calculation with the Rock-Eval pyrolysis, and the T_{max} cannot show true thermal maturity level. According to the uncorrected T_{max} data from the Rock-Eval in the locations of A and C, the Garau Formation in these locations is in the immature stage. But the real maturity will be higher and is in the mature stage.

The richness of samples from organic carbon (high TOC), has led to adsorption of heavy bitumen on organic matter rich facies of the Garau Formation, subsequently the in-situ contamination has occurred, and the generated hydrocarbons didn't expel. Also, the diagram of B, D, and E locations show slightly x-intercept due to mineral matrix effect (Langford and Valleron, 1990). After correcting with above mentioned formula, the real geochemistry parameters were obtained and compared with calculated data from the Rock-Eval pyrolysis in the tables 2 and 3.

4.2. The S₂ versus TOC diagram

The cross-plot of HI versus TOC reveals indigenous relation between products and organic matter contents (Figure 4). So that, the HI apparently increased with increase of the TOC. The regression line

demonstrates how the HI going up with the increasing of TOC. Also, based on the almost similar trend between HI and TOC data, the products are mainly coming from a same origin. However, the figure shows an irrational relationship between HI versus TOC for significant number of samples, so that, the high HI obtained from the low TOC contents. Meaning high bitumen/hydrocarbon produced from lower organic matter contents. On the other hand, the regression line in the S_2 versus TOC cross-plot in the A and C location samples doesn't pass through the origin (Figure 5). Another irrational situation established in the location samples of B, D, and E, where due to the mineral matrix effect in adsorbing of hydrocarbons, the lower HI has derived from the higher TOC (Langford and Valleron, 1990; Dahl et al., 2004).

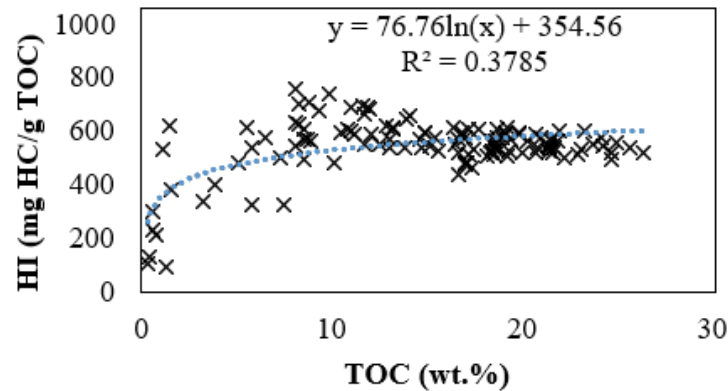
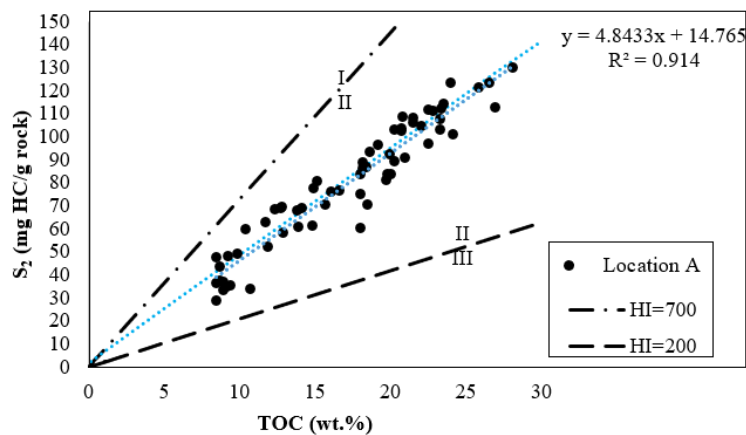
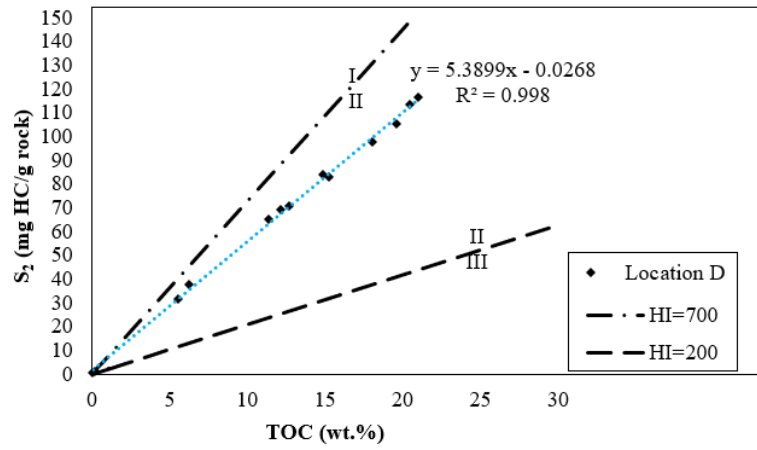
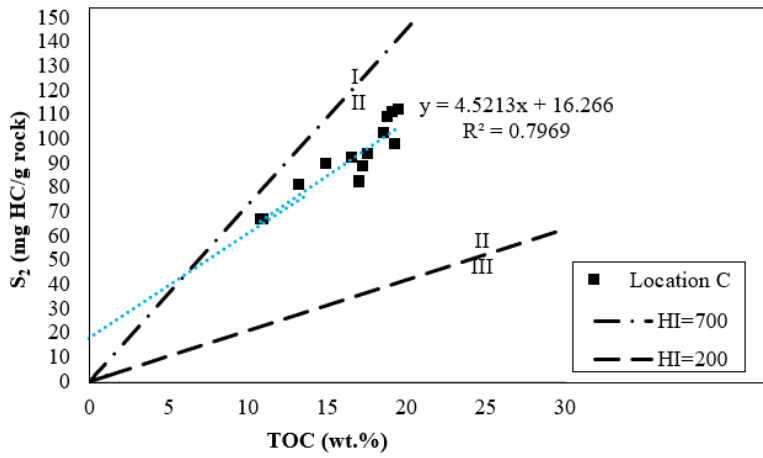
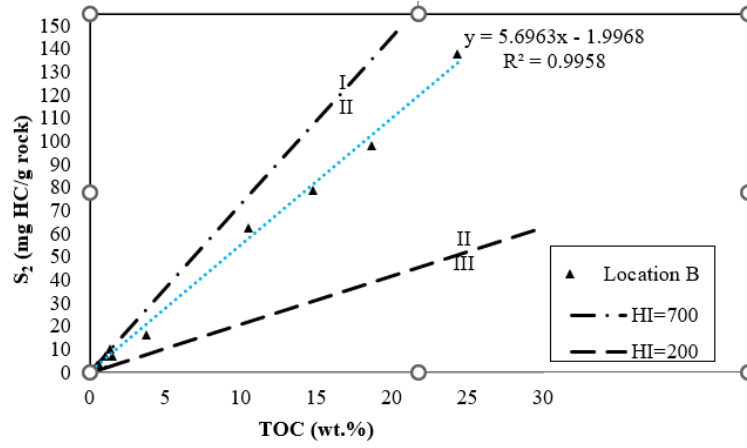


Figure 4

The HI versus TOC cross-plot to investigate relationship between products and organic matter.





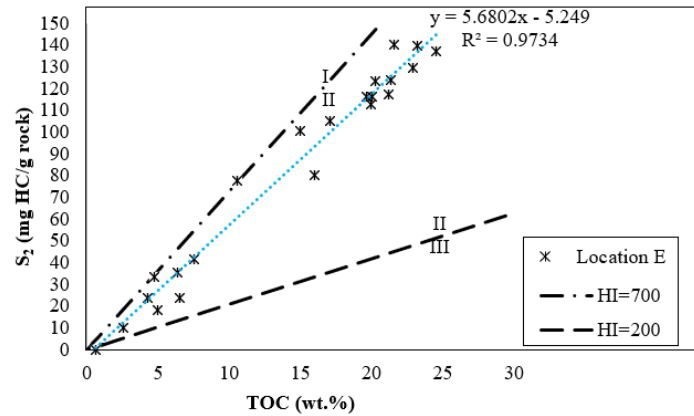


Figure 5

The S2 versus TOC cross-plot indicate y-intercept in locations A and C, showing bitumen contamination (Langford and Valleron, 1990).

Since the HI versus OI cross-plots (Figure 3) doesn't show the presence of inert kerogen, whereas reveals the oil-prone kerogens, then the x-intercept in the B, D, and E locations created by the mineral matrix effect. Nevertheless, according to the regression line for all data plot in the figure 5, the samples affected by the matrix effect are very lower than the contaminated samples. As well as, the two agents can be detected for creating that abnormal situation in the A and C locations; first is the in-situ bitumen contamination in the source rock, and the second reason is immigration to the source rock. According to the figure 6, the free hydrocarbons (S1) are indigenous and produced by maturation of the organic matter of the source rock, and no external agent such as immigration interfered in contamination of the Garau Formation (Espitalie et al., 1977; Hunt, 1996). The covalent bonding between hydrogen and carbon ions in the heavy bitumen of the Garau Formation caused the generated products to adhere the surface of organic facies. Then, the heavy bitumen remains in the source rock even at high temperatures and have not expelled easily. Eventually, the in-situ contamination has occurred (Morrison and Boyd, 1992; Mortimer, 1986).

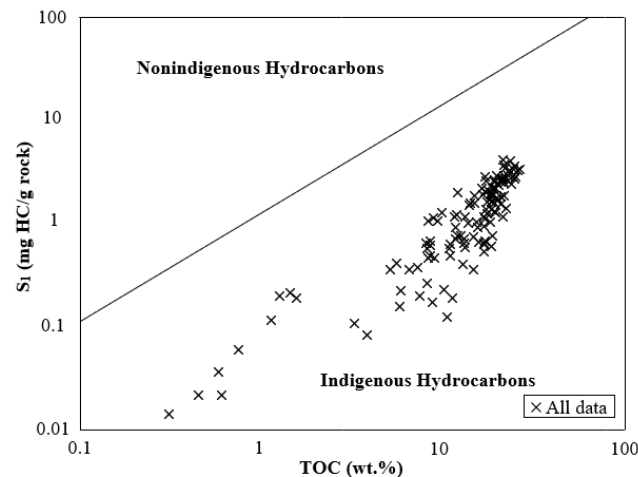


Figure 6

S1 versus TOC cross-plot, to find out migration from immigration (Hunt, 1996).

The calculated HI from contaminated samples by the Rock-Eval pyrolysis and without making any appropriate corrections, usually are not represent the true HI. Such uncorrected data will induce scattered plots and interception on the Y-axis in the graphs of HI versus TOC, and S2 versus TOC. The

y-intercept when induced that the samples with high HI or S₂ associated with low TOC. The contamination caused the S₂ and HI values to increase unrealistically, and to decrease the T_{max} from its real values (Peters, 1986). In such situations, the thermal maturation occurs earlier and the peak of S₂ appears more easily. Then, the real thermal maturity in the contaminated samples will be higher than calculation with the Rock-Eval pyrolysis, and the T_{max} cannot show true thermal maturity level. According to the uncorrected T_{max} data from the Rock-Eval in the locations of A and C, the Garau Formation in these locations is in the immature stage. But the real maturity will be higher and is in the mature stage.

The richness of samples from organic carbon (high TOC), has led to adsorption of heavy bitumen on organic matter rich facies of the Garau Formation, subsequently the in-situ contamination has occurred, and the generated hydrocarbons didn't expel. Also, the diagram of B, D, and E locations show slightly x-intercept due to mineral matrix effect (Langford and Valleron, 1990). After correcting with above mentioned formula, the real geochemistry parameters were obtained and compared with calculated data from the Rock-Eval pyrolysis in the tables 2 and 3.

Table 2

Description of kerogen type and measuring geochemistry parameters by the Rock-Eval pyrolysis.

Sampling location	Kerogen type	Mean HI mg HC/g TOC	Mean S ₂ mg HC/gr rock	Mean S ₂ /S ₃
Location A	I	588.0 (Range:442-762)	91.7 (Range:44.5-138.7)	92.9 (Range:21.7-289.6)
Location B	I/II	449.3 (Range:213-621)	38.4 (Range:1.4-139.6)	30.6 (Range:4.7-77.5)
Location C	I	555.2 (Range:479-611)	90.5 (Range:66-111.6)	61.9 (Range:23.4-106.2)
Location D	II	478.7 (Range:106-576)	67.0 (Range:0.3-115.9)	61.9 (Range:0.4-126.4)
Location E	I/II	497.0 (Range:93-667)	82.6 (Range:1.2-140.2)	73.2 (Range:1.7-222.5)

Table 3

Real geochemical parameters after correction.

Sampling Location	Kerogen type	Mean HI mg HC/g TOC	Mean S ₂ mg HC/gr rock	Mean S ₂ /S ₃
Location A	I	484.11 (Range:340-593.39)	77.00 (Range:29.8-124)	78.07 (Range:14.55-253.76)
Location B	I/II	583.58 (Range:455.61-759.03)	40.30 (Range:3.4-141.6)	34.45 (Range:10.56-78.64)
Location C	I/II	452.52 (Range:383-495.26)	74.3 (Range:49.7-95.4)	50.81 (Range:18.71-90.27)
Location D	I	479.59 (Range:112.9-576.23)	67.0 (Range:0.4-115.9)	61.87 (Range:0.44-126.37)
Location E	I/II	561.97 (Range:400.54-712.19)	87.9 (Range:6.4-145.4)	77.74 (Range:9.03-230.84)

On the basis of S₂ versus TOC cross-plots, the organic characteristics and hydrocarbon generation potential are almost similar in all locations. Regarding the geochemistry parameters of S₂/S₃, HI and

TOC, the Garau Formation is predominantly considered as a good to excellent source rock which formed mainly from kerogen type II, and some I and III, with main expelled products of oil or gas mixed oil (Hunt, 1996; Jarvie, 1991).

5. Other applications

The S₂ versus TOC cross-plots have been used to determine the depositional system tracts (Dahl et al., 2004; Maky et al., 2010; Phiri et al., 2014). The S₂ versus TOC cross-plots were applied in determining the deposition environment of the rock samples. Current study's data compared with research of Robison and Engel (Robison and Engel, 1993) about usage of cross plot of S₂ versus TOC in analysing the transgressive system tracts (TST) and high stand system tracts (HST) of the Late Cretaceous age in Egypt (Figure 7). The TST form smooth low angle (larger amounts of oil-prone organic carbon) close to linear trend whilst the HST form large and steeper angle (more gas-prone organic carbon) with a more chaotic distribution pattern. The TST is characterized by rise in the sea level, lower terrestrial, and reworked organic matter (with higher HI values) entering the basin. Sediments are supplied mostly from the basin. The HST is supported by the higher average amount of TOC and the low values of pyrolysable HI and the scattered plot pattern suggesting that the organic material was derived from terrestrial and reworked materials that are typically gas-prone. While the TST characterized by higher HI derived from higher TOC in a linear pattern. So, the clues prove the Garau Formation sedimented under anoxic conditions during sea level rise or transgression (Bordenave, M. L., and Burwood, 1990; Haq et al., 1987; Sarfi et al., 2015).

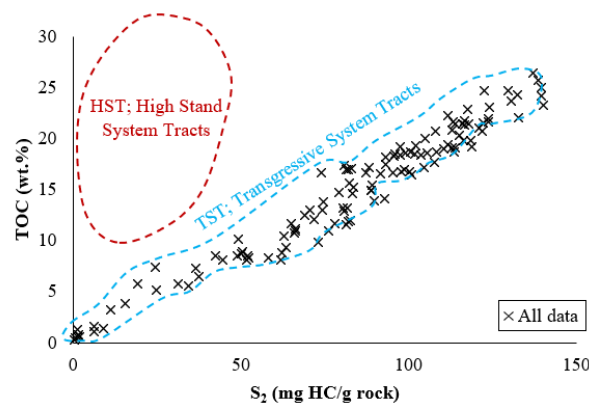


Figure 7

haracterization of sedimentary system tracts of Garau Formation using S₂ versus TOC parameters (modified after Dahl et al., 2004; Robison and Engel, 1993)

6. Conclusion

The adsoption of heavy bitumen to organic-rich facies prevents the easy expulsion of hydrocarbons, and caused the in-situ bitumen contamination. The S₂ versus TOC cross-plots are a criterion accuracy of geochemistry parameters and complement to the Rock-Eval uncertainties. Accordingly, after drawing regression line, the y-intercept was seen in the contaminated samples of two locations (A and C), which caused overestimation in the S₂ and HI values. In order to eliminate the effect of contamination on the geochemistry parameters, the following formula offered:

$$\text{Real } S_2 = S_2 - Y_{\text{intercept}} \quad (7)$$

$$\text{Real HI} = \text{Real S2} / \text{TOC} \times 100 \quad (8)$$

$$\text{Real PI} = \text{S1} / (\text{S1} + \text{Real S2}) \quad (9)$$

In the three locations where the x-intercept induced by the mineral matrix effect (B, D, and E), the real S2 obtained according to the following formula:

$$\text{Real S2} = \text{S2} + \text{yintercept} \quad (10)$$

Due to the effect of contamination and underestimation in the Tmax values, this parameter couldn't be reliable for thermal maturity evaluations. Therefore, to access the thermal maturity, other parameters such as vitrinite reflectance or biomarkers should be applied.

Other applications of the S2 versus TOC graph include providing information on the depositional system tract. This method illustrates the Garau Formation is a type of HST system tract.

Nomenclatures

TOC: total organic carbon, wt. %

HI: hydrogen index, mg HC/gr TOC

OI: oxygen index, mg CO₂/g TOC

PI: production index, mg HC/g rock

TST: transgressive system tract

HST: high stand system tract

References

- Alavi, M., Regional Stratigraphy of the Zagros Fold-Thrust Belt of Iran and Its Proforeland Evolution, *American Journal of Science*, Vol. 304, No. 1, p. 1-20, 2004.
- Al-Husseini, And Moujahed I., Origin of The Arabian Plate Structures: Amar Collision and Najd Rift, *GEOARABIA-MANAMA*, Vol. 5, No. 4, P. 527-542, 2000.
- Bernard, Bernie B., Heather, B., And James, M., B., Determination of Total Carbon, Total Organic Carbon and Inorganic Carbon in Sediments, College Station, Texas, P. 1-5, 2010.
- Bordenave, M. L., *Applied Petroleum Geochemistry*, Paris, Editions Technip, Organic Geochemistry, Vol. 21, P. 524, 1993.
- Bordenave, M. L., And Burwood, R., Source Rock Distribution and Maturation in The Zagros Orogenic Belt: Provenance of The Asmari and Bangestan Reservoir Oil Accumulations, *Organic Geochemistry*, Vol. 16, NO. 1, P. 369-387, 1990.
- Bordenave, M. L., And Hegre, J. A., Current Distribution of Oil and Gas Fields in The Zagros Fold Belt of Iran 424 And Contiguous Offshore as The Result of The Petroleum Systems, Geological Society, London, Special Publications, Vol. 330, P. 291-353, 2010.

- Bordenave, M. L., And Hegre, J. A., The Influence of Tectonics on The Entrapment of Oil in The Dezful Embayment, Zagros Foldbelt, Iran, *Journal of Petroleum Geology*, Vol. 28, No. 4, P. 339-368, 2005.
- Clayton J. L., And Ryder, R. T., Organic Geochemistry of Black Shales and Oils in The Minnelusa Formation (Permian and Pennsylvanian), Powder River Basin, Wyoming, In Woodward J, Meissner F. F, Clayton J. L. (Eds.), *Hydrocarbon Source Rocks of The Greater Rocky Mountain Region*, Denver, Rocky Mountain Association of Geologists, P. 231-253, 1984.
- Dahl, B., Bojesen-Koefoed, J., Holm, A., Justwan, H., Rasmussen, E., And Thomsen, E., A New Approach to Interpreting Rock-Eval S2 And TOC Data for Kerogen Quality Assessment, *Organic Geochemistry*, Vol. 35, No. 11-12, P. 1461-1477, 2004.
- Erik, N. Y., Özçelik, O., And Altunsoy, M., Interpreting Rock–Eval Pyrolysis Data Using Graphs of S2 Vs. TOC: Middle Triassic–Lower Jurassic Units, Eastern Part of SE Turkey, *Journal of Petroleum Science and Engineering*, Vol. 53, No. 1-2, P. 34-46, 2006.
- Espitalié, J., Deroo, G., And Marquis, F., La Pyrolyse Rock-Eval Et Ses Applications, Partie I, *Revue De l'Institut Français Du Pétrole*, Vol. 40, No. 5, P. 563-579, 1985a.
- Espitalié, J., Deroo, G. And Marquis, F., La Pyrolyse Rock-Eval Et Ses Applications, Partie II, *Revue De l'Institut Français Du Pétrole*, Vol. 40, No. 6, P. 755-784, 1985b.
- Espitalie, J., Madec, M., Tissot, B., Menning, J. J., And Leplate, P., Source Rock Characterization on Method for Petroleum Exploration, *Proceeding of the 9th Annual Offshore Technology Conference*, Houston, P. 439-444, 1977.
- Ghazban F., And Motiei H., *Petroleum Geology of The Persian Gulf*, Tehran University and National Iranian Oil Company, Tehran, P. 722, 2007.
- Haq, B. U., Hardenbol, J. A. N., And Vail, P. R., Chronology of Fluctuating Sea Levels Since the Triassic, *Science*, Vol. 235, No. 4793, P. 1156-1167, 1987.
- Homke, S., Vergés, J., Serra-Kiel, J., Bernaola, G., Sharp, I., Garcés, M., Montero-Verdú, I., Karpuz, R. And Goodarzi, M.H., Late Cretaceous–Paleocene Formation of The Proto–Zagros Foreland Basin, Lurestan Province, SW Iran, *Geological Society of America Bulletin*, Vol. 121, No. 7-8, P. 963-978, 2009.
- Hunt, J. M., *Petroleum Geochemistry and Geology*, 2nd Ed. W. H. Freeman and Company, New York, P. 743, 1996.
- Jarvie, D. M., *Total Organic Carbon (TOC) Analysis: Chapter 11: Geochemical Methods and Exploration*, P. 113-118, 1991.
- Langford, F. F., And Blanc-Valleron, M. M., Interpreting Rock-Eval Pyrolysis Data Using Graphs of Pyrolizable Hydrocarbons Vs. Total Organic Carbon (1), *AAPG Bulletin* Vol. 74, No. 6, P. 799-804, 1990.
- Maky, A. F., Ahmad, S., And Mousaand, N. I. M., Source Rock and Paleoenvironmental Evaluation of Some Pre-Rift Rock Units at The Central Part of The Gulf of Suez, Egypt. *J. Appl. Sci. Res*, Vol. 6, No. 5, P. 51, 2010.
- Miller, R. G., A Future for Exploration Geochemistry, In: Grimalt, J. O., Dorronsoro, C. (Eds.), *Organic Geochemistry: Developments and Applications to Energy, Climate, Environment and Human History*, A.I.G.O.A., Donostia-San Sebastia´ N, Spain, P. 412-414, 1995.
- Morrison, R. T., And Boyd, R. N., *Organic Chemistry*, 6th Ed, Prentice Hall, P. 1279, 1992.

- Mortimer, C. E., *General Chemistry*, 6th Ed, Wadsworth Publishing Company, P. 902, 1986.
- Motiei, H., *Treatise on The Geology of Iran: Stratigraphy of Zagros*, Geological Survey of Iran, Tehran, P. 497 (In Persian), 1993.
- Peters, K. E., And Cassa, M. R., *Applied Source Rock Geochemistry*, In: Magoon, L. B., Dow, W. G. (Eds.), *The Petroleum System—From Source to Trap*, AAPG, P. 93-120, 1994.
- Peters, K. E., And Fowler, M. G., *Application of Petroleum Geochemistry to Exploration and Reservoir Management*, *Organic Geochemistry*, Vol. 33, P. 5-36, 2002.
- Peters, K. E., *Guidelines for Evaluating Petroleum Source Rock Using Programmed Pyrolysis*, *Am. Assoc. Pet. Geol.*, Vol. 70, No. 3, P. 318-329, 1986.
- Phiri, C., Pujun, W. A. N. G., Nguimbi, G. R., And Hassan, A. Y. I., *Interpreting Effects of Tocinert Organic Content on Source Rock Potential Using S2 Vs. TOC Graph in Maamba Coalfield, Southern Zambia*, *Global Geology*, Vol. 17, No. 4, P. 199-205, 2014.
- Rimmer, S. M., Cantrell, D. J., And Gooding, P. J., *Rock-Eval Pyrolysis and Vitrinite Reflectance Trends in The Cleveland Shale Member of The Ohio Shale, Eastern Kentucky*, *Organic Geochemistry*, Vol. 20, No. 6, P. 735-745, 1993.
- Robison, V. D., And Engel, M. H., *Characterization of The Source Horizons with In the Late Cretaceous Transgressive Sequence of Egypt*, *AAPG Studies in Geology*, Vol. 37, P. 101-117, 1993.
- Sarfi, M., Ghasemi-Nejad, E., Mahanipour, A., Yazdi-Moghadam, M., And Sharifi, M., *Integrated Biostratigraphy and Geochemistry of The Lower Cretaceous Radiolarian Flood Zone of The Base of The Garau Formation, Northwest of Zagros Mountains, Iran*, *Arabian Journal of Geosciences*, Vol. 8, No. 9, P. 7245-7255, 2015.
- Thomas, G. B., Weir, M. D., Hass, J., Heil, C., And Behn, A., *Thomas' Calculus: Early Transcendentals*, 13th Edition, Boston, Pearson, 2016.
- Tissot, B. P., And Welte, D. H., *Petroleum Formation and Occurrence*. 2nd Ed. Springer-Verlag Berlin Heidelberg, P. 702, 1984.
- Tyson, R.V., *Sedimentary Organic Matter: Organic Facies and Palynofacies*, Chapman and Hall, London, P. 615, 1995.
- Wynd, J. G., *Biofacies of The Iranian Consortium-Agreement Area*, Iranian Oil Operating Companies Report 1082 (Unpublished), 1965.

**COPYRIGHTS**

©2022 by the authors. Licensee Iranian Journal of Oil & Gas Science and Technology. This article is an open access article distributed under the terms and conditions of the Creative Commons Attribution 4.0 International (CC BY 4.0) (<https://creativecommons.org/licenses/by/4.0/>)